

## Flow topology around two square cylinders in side-by-side arrangement

Md. Mahbub Alam<sup>1,\*</sup> and Y. Zhou<sup>1,2</sup>

<sup>1</sup> Institute for Turbulence-Noise-Vibration Interaction and Control, Shenzhen Graduate School, Harbin Institute of Technology, Shenzhen, China

<sup>2</sup> Department of Mechanical Engineering, The Hong Kong Polytechnic University  
Hung Hom, Kowloon, Hong Kong

E-mail: [alamm28@yahoo.com](mailto:alamm28@yahoo.com)

### Abstract

The wake of two side-by-side square cylinders is experimentally investigated in details at a Reynolds number of 300 to explore its intrinsic features, including the gap vortices, flow switch, stability, merging of two streets into one, etc. The cylinder center-to-center spacing ratio  $T^*$  ( $= T/W$ ,  $W$  is the cylinder width) is varied from 1.0 to 5.0. Four flow regimes are identified: (i) the single bluff body regime ( $T^* < 1.2$ ), (ii) the narrow and wide street regime ( $1.2 < T^* < 2.1$ ), (iii) the transition regime ( $2.1 < T^* < 2.4$ ), and (iv) the coupled-street regime ( $T^* > 2.4$ ). At Regimes (ii) and (iii), the two opposite-signed vortices separated from the gap side of the cylinders behave like a conjoined twin and tend to move together. Their movement direction depends on the phase lag between them. Two streets formed immediately behind the cylinders merge to a single street at a downstream location  $x_c^*$  that depends on  $T^*$ . A larger  $T^*$  corresponds to a larger  $x_c^*$ . Regime (iv) is characterized by two streets either inphased or antiphased. The antiphased streets are more stable than the inphased.

Keywords: flow topology, bistable flow, square cylinders, side-by-side arrangement.

### 1. Introduction

The wake of two side-by-side cylinders has attracted a great deal of attention in the literature because of its fundamental importance in understanding many industrial flows, for example, flows around high-rise buildings, chimney stacks, tubes in heat exchangers, overhead power-line bundles, bridge piers, stays, masts, chemical-reaction towers and offshore platforms, etc. The vortex shedding process, gap flow switch, vortex and street interactions are the key features of this flow, which are complicated and fascinating. These phenomena are strongly dependent upon the cylinder center-to-center spacing ratio  $T^*$ . Superscript ‘\*’ denotes normalization by the cylinder width  $W$ . They are further linked to the downstream evolution of vortex frequencies and dramatic change in forces and pressure distributions on each cylinder [1, 2].

In spite of its great relevance to engineering, the flow around two square cylinders has received much less attention than that around two circular cylinders. Sakamoto and Haniu [3] investigated aerodynamic forces, Strouhal number ( $St$ ) and cross-correlation between fluctuating pressures on two side-by-side square cylinders, with an aspect ratio of 3, immersed in a thick turbulent boundary layer. They failed to observe the bistable phenomenon of the gap flow. Using a two-component laser Doppler velocimeter, Kolar et al.

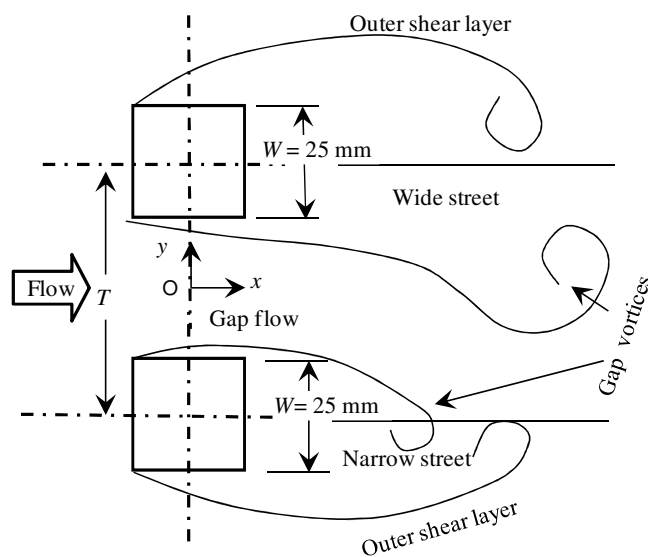
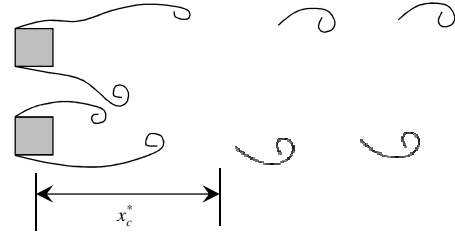


Fig. 1. Schematic of cylinders and definitions of symbols

[4] measured the wake of two side-by-side square cylinders at a Reynolds number ( $Re$ ) of  $2.3 \times 10^4$  over  $x^* = 1 \sim 9$ , where  $x$  is the streamwise distance from the cylinder centers (Fig. 1). The flow was studied in detail only at  $T^* = 3$ , providing no information on flow in other  $T^*$ . Agarwal et al. [5] investigated the laminar wake ( $Re = 73$ ) of two side-by-side square cylinders at  $T^* = 1.7$  and 3 numerically using a lattice Boltzmann method. They observed coupled vortex shedding from the two cylinders at  $T^* = 3$ , and a biased gap flow at  $T^* = 1.7$ . The gap flow could switch randomly from one side to the other, forming narrow and wide streets behind the cylinders. The two streets are connected to different vortex shedding frequencies.

The flow structure in the narrow and wide streets is complicated by the gap flow switch, which may have a timescale of several orders of magnitude longer than those of vortex shedding and shear layer instability. The two streets, generated by the two cylinders, respectively, merge into one single large-scale street (Fig. 2). The flow physics behind the merging has yet to be completely understood. It is expected that the downstream position where the two streets merge should be dependent on  $T^*$  in addition to other parameters such as  $Re$ , turbulent intensity, etc. However there is no quantitative information available in relation to this aspect. Other aspects of the flow are also interesting. For example, why is the gap flow biased? Under what condition does the deflected gap flow switch to the other side? What kind of vortex interactions is associated with the gap flow switch? How do the two streets evolve into a single one? The issues raised above motivate this work. In order to capture the flow structure details of interest, the present investigation is conducted at a low  $Re$  of 300 for  $T^* = 1.0 \sim 5.0$  based on laser-induced fluorescence flow visualization. Various aspects of the flow are carefully examined, including vigorous interactions between gap vortices, non-stationary gap flow switching, downstream flow evolution and changeover from the antiphased to inphased coupled streets or vice versa



**Fig. 2.** Two streets merge into one.

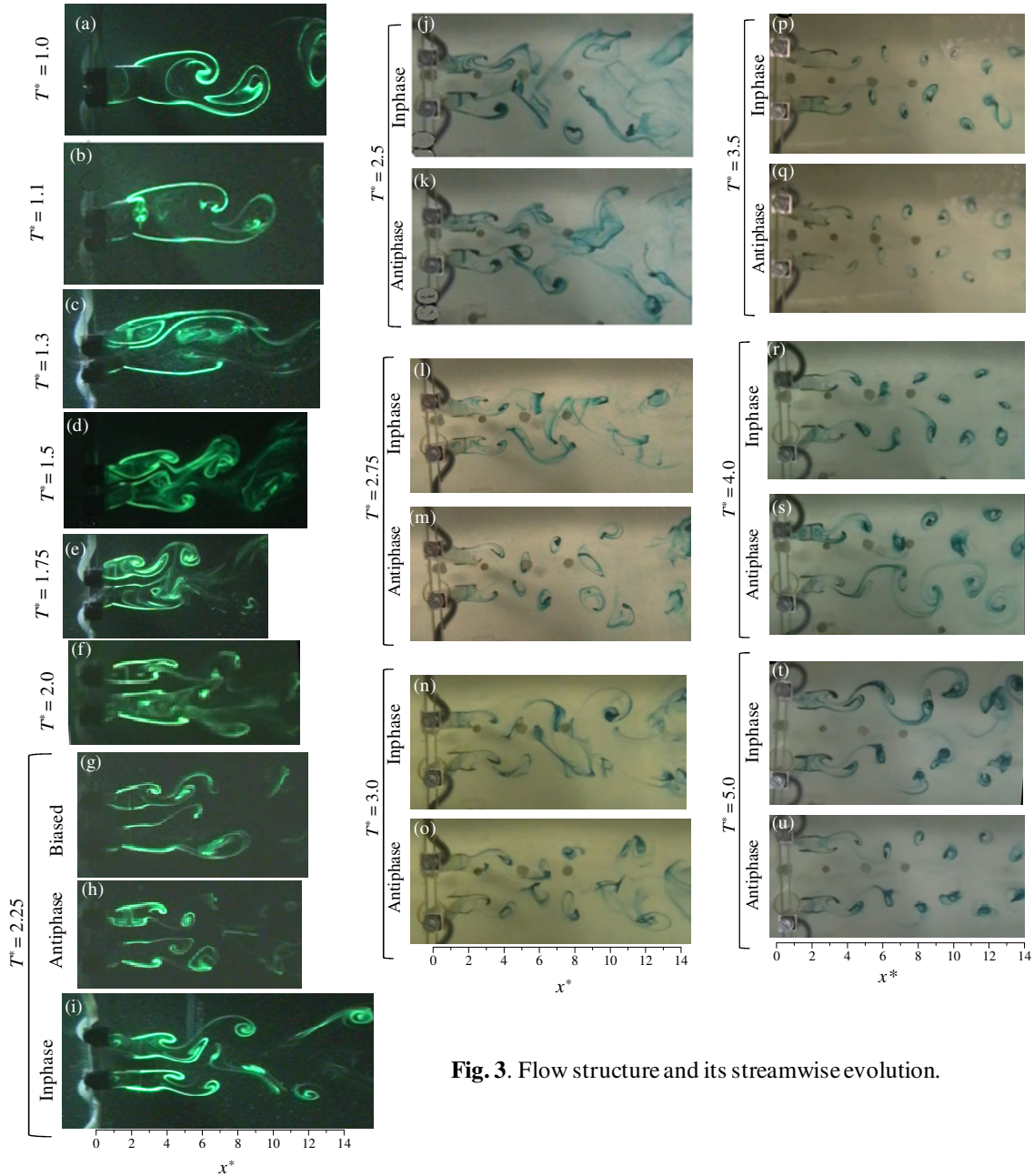
## 2. Experimental details

Figure 1 presents the schematic of the cylinder arrangement, along with the definitions of symbols. The Cartesian coordinate system is defined such that the origin is at the midpoint between the two cylinders, with the  $x$ - and  $y$ -axis along the streamwise and lateral directions, respectively. Flow visualization experiments were conducted in a water tunnel in the Department of Mechanical Engineering at The Hong Kong Polytechnic University. The test section is rectangular, 0.3 m in width, 0.6 m in height, and 2.0 m in length. Two square cylinders of  $W = 25$  mm were arranged side-by-side and mounted vertically across the height of the tunnel. Flow visualization was performed at the free-stream velocity  $U_\infty = 0.012$  m/s, corresponding to  $Re = 300$ . Dye (Rhodamine 6G 99%) was introduced into flow from the midspan of the cylinders through three pinholes (spaced 2 mm) at each leading edge. A thin laser sheet, generated by laser beam sweeping, provided illumination in the vertical plane through the mid-span of the cylinders. A Spectra-Physics Stabilite 2017 Argon Ion laser (4 watts) was used to generate the laser beam. A digital video camera was used to record the dye-marked vortex street at a framing rate of 25 frames per second. Experiments were done for  $T^* = 1.0, 1.1, 1.3, 1.5, 1.75, 2.0, 2.25, 2.5, 2.75, 3.0, 3.5, 4.0,$  and 5.0.

## 3. Results and discussion

### 3.1. Flow structure and its downstream evolution

Figure 3 presents the flow structure and its downstream evolution for various  $T^*$ . There is no flow through the gap at  $T^* = 1.0$  (Fig. 3a) and the gap bleeding is hardly discernible at  $T^* = 1.1$  (Fig. 3b). In both cases, a single street of vortices forms, characterized by alternate vortex shedding from the free-stream sides of the cylinders. The corresponding  $St$  is about one half of that in an isolated cylinder wake, as the effective bluff-body width is doubled. As  $T^*$  is increased to 1.3, the gap flow grows to a strength enough to split the wake into two streets (Fig. 3c). Nonetheless, with insufficient momentum, the gap flow swerves aside, forming one narrow and one wide street (Fig. 3c). The gap flow rolls up, forming two oppositely signed vortices; both running into the narrow street. The narrow street has a smaller vortex formation length than the wide one. The two streets have their identities at  $x^* < 3.8$ , though merging into one street at the critical distance  $x_c^* = 3.8$  for  $T^* = 1.3$  and displaying only two rows of vortices. For larger  $T^*$ , up to  $T^* = 2.0$  (Fig. 3d-f), the gap flow grows in momentum and becomes gradually less biased, the difference in width between the narrow and wide streets diminishing. However, the two streets merge into one in the downstream. It may be concluded that a single bluff-body wake occurs at  $T^* < 1.2$  but one narrow and one wide street are generated for  $1.2 < T^* < 2.1$ .



**Fig. 3.** Flow structure and its streamwise evolution.

At  $2.1 < T^* < 2.4$ , four distinct flow structures are identified, viz., with the gap flow biased downward (Fig. 3g), biased upward (not shown) and unbiased that may form antiphased and inphased vortex streets (Fig. 3h-i), respectively. Furthermore, they may switch from one to another. While the inphased or antiphased vortex shedding occurs only for a few cycles, the biased gap flow comes into view mostly with a switch of the gap flow in every cycle. At  $T^* = 2.4 \sim 3.25$ , both inphased and antiphased flow structures are observed (Fig. 3j-o). Two symmetric or anti-symmetric streets (four rows of vortices) may merge into one single street (two rows of vortices) in the downstream. The observation implies that the four rows of vortices are not yet stable at this  $T^*$  range, probably because of appreciable interactions between vortices, especially between the two inner rows. It is noted that  $x_c^*$  increases for larger  $T^*$ . In other words, the stability of the streets is enhanced at large  $T^*$ . This is reasonable in view of the weakened interaction between the streets at larger  $T^*$ . Another notable feature is that the antiphased streets are stable for a longer  $x_c^*$  than the inphased. For example, the two inphased streets at  $T^* =$

2.5, 2.75, and 3.0 persist up to  $x_c^* = 6.23, 8.0, \text{ and } 11.2$ , respectively, but the antiphased only up to  $x_c^* = 9.13, 10.5, 12.6$ , respectively (see Fig. 3j-o). These  $x_c^*$  values have been estimated based on an average of more than 20 flow images for each  $T^*$ . With a further increase in  $T^*$  up to 5.0, inphased or antiphased shedding occurs and persists for the entire  $x^*$  range of the image. That is, the two streets are stable at least up to  $x^* = 14$ . Figure 4 shows how  $x_c^*$  varies with  $T^*$ . It is noted that  $x_c^*$  increases rapidly with  $T^*$  for  $T^* > 2.2$ , where the two streets are initially either inphased or antiphased, but slowly for  $T^* < 2.2$ , where the narrow and wide streets are generated. The inflection point occurs at  $T^* = 2.2$  that nestles in the transition regime. An inflection point is mathematically a point where curvature changes from positive to negative or vice versa. In other words, the variation of  $x_c^*$  with  $T^*$  follows a third order polynomial, viz.

$$x_c^* = -38.18 + 59.50T^* - 26.82T^{*2} + 4.21T^{*3}, \quad (T^* > 1.2). \quad (1)$$

Eq. (1) is obtained by curve fitting to the data in Fig 4. The inflection point of Eq. (1) occurs at  $T^* = 2.15$ , which is very close to  $T^* = 2.2$  observed physically.

The results and discussion presented above lead to the classification of flow into four regimes: (i) the single bluff body regime ( $T^* < 1.2$ ) where flow through the gap is feeble to split the wake into two streets, (ii) the asymmetric wake regime ( $1.2 < T^* < 2.1$ ) where the gap flow splits the wake into one narrow and one wide street, (iii) the transition regime ( $2.1 < T^* < 2.4$ ) where both the asymmetric wake and the coupled streets in an inphase or antiphase mode occur, and (iv) the coupled-street regime ( $T^* > 2.4$ ) where the streets are inphase- or antiphase-coupled. The inflection point at  $T^* = 2.2$  in the transition regime separates the asymmetric wake and the coupled-street regimes.

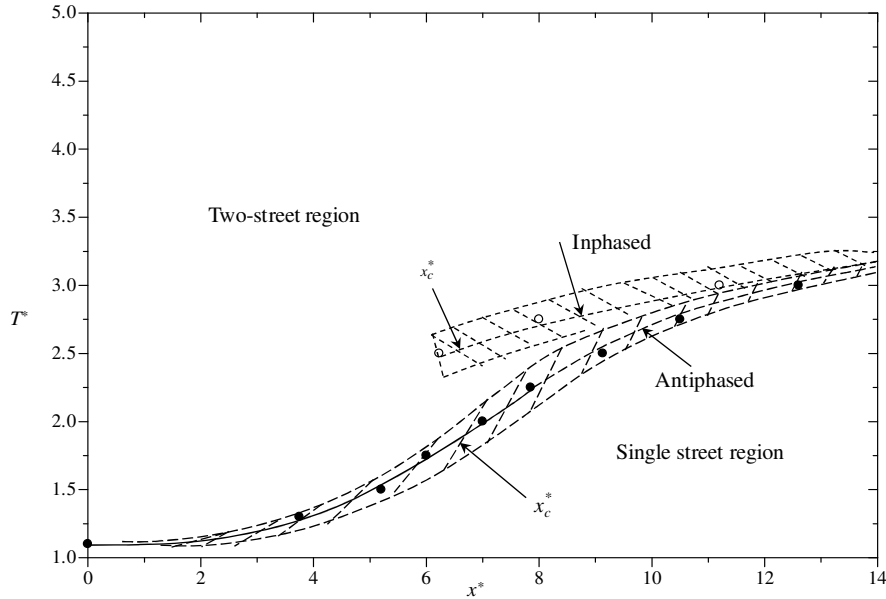


**Fig. 4.** Dependence of the critical  $x_c^*$  on  $T^*$ , at which the two streets merge into one.

### 3.2. Mechanism of the gap flow bias

The gap flow separates from the inner side of the cylinders and rolls up to form two counter-rotating vortices  $E$  and  $F$ , respectively (Fig. 5a). Assume the two cylinders are symmetrically arranged with respect to approaching flow in the working section. Vortices  $E$  and  $F$  should go to the upper and lower streets, respectively. That does not happen of course. Both vortices behave like a conjoined twin and tend to move together. Why? Since the two vortices shed from the gap, the initial lateral distance between them depends on  $T^*$ . The larger the  $T^*$ , the greater is the lateral spacing between them. At sufficiently small  $T^*$ , the two opposite-signed vortices (Fig. 5b) are adequately close, and the flow between them accelerates because of the same-signed velocities, resulting in a low pressure region between. As such, the two vortices attract each other when advected and tend to move together. The low pressure between them is a tie between the conjoined twin. Couder and Basdevant [6] examined experimentally and numerically the convective behaviors of two coupled vortices of opposite sign and

two of the same sign. They found that the coupled vortices of opposite sign moved faster than those of the same sign. Furthermore, the flow velocity across the gap is highest at the centerline, which also contributes to the low pressure between the gap vortices. Presumably, both streets have the same pressure, then the direction the twin move is crucial. As sketched in Fig. 5(b), their resultant direction will be that of the velocity at their interface, which is dependent on the phase difference between the vortices. The resultant direction will be inclined downward if  $E$  leads  $F$ , and upward if  $E$  lags  $F$ . The leading and lagging may happen naturally or may be governed by the pressure difference between the streets.

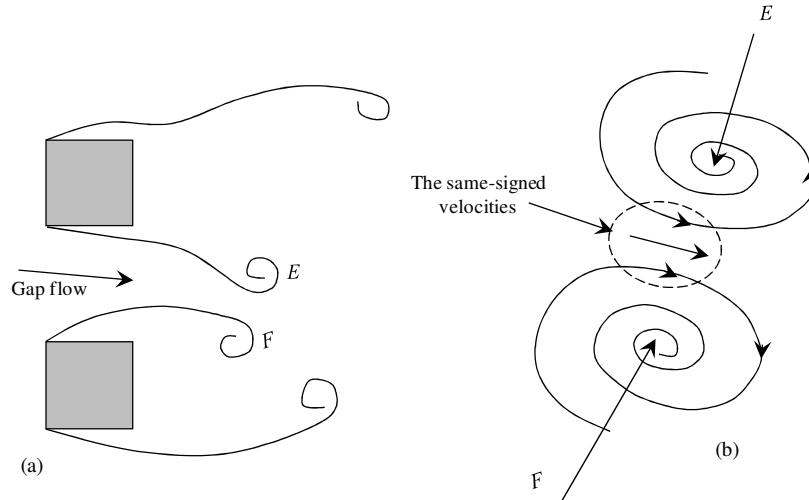


**Fig. 5.** (a) Counter-rotating gap vortices. (b) Generation of larger velocities and lower pressure between two counter-rotating vortices.

### 3.3. Evolution of two streets into one

The merge of the wide and narrow streets into one has been shown in Fig. 3(a-f). It is of great interest to understand how two inphase- or antiphase-coupled streets evolve to a single street. Figure 6 shows typical sequential photographs and corresponding sketches to illustrate the process. The real time index (minute : second : frame-number) is shown on the upper left corner of each plate. Two separate streets are initially generated, each consisting of two rows of vortices. As the vortices are advected downstream, the upper inner vortex  $E$  trips to the lower street and comes close to  $F$  (Fig. 6b). It has been discussed earlier that the two vortices separated from the gap tend to stay together because of the low pressure region between them. Vortex  $E$ , which leads  $F$ , wanders toward the lower street. Once coming close, they accelerate and their speeds increase, catching up with vortex  $G$ . With the same sense of rotation,  $E$  and  $G$  merge first and keep  $F$  in abreast (Fig. 6c). Eventually,  $E$ ,  $F$  and  $G$  amalgamate, forming a big anti-clockwise vortex. This vortex and clockwise vortex  $D$  in the initial upper street form a stable single street.

## 4. Conclusions

A detailed study has been conducted of the flow structure, gap flow switch and stability in the wake of two side-by-side square cylinders at  $Re = 300$  based on flow visualization data. The examined  $T^*$  is from 1.0 to 5.0.

Four flow regimes are identified, namely (i) single bluff body regime ( $T^* < 1.2$ ) where the gap flow momentum is feeble to split the wake into two streets, (ii) asymmetric wake regime ( $1.2 < T^* < 2.1$ ) where the gap flow having sufficient momentum splits the wake into one narrow and one wide street, (iii) transition regime ( $2.1 < T^* < 2.4$ ) where both the asymmetric wake and the coupled streets in an inphase or antiphase mode presist, and (iv) coupled-street regime ( $T^* > 2.4$ ) where the two streets are inphase- or antiphase-coupled.

One explanation is provided on why the flow through the gap is biased in the asymmetric wake regime, forming the narrow and wide streets. The two oppositely signed gap vortices behave like a conjoined twin and tend to move together. A low pressure region is generated due to the same signed and hence larger velocities between the vortices, which acts to maintain the two vortices together and even closer during their advection. The phase lag between the gap vortices holds the key for the destination street the two gap vortices will join. The two

streets always merge to one at  $x_c^*$ , which depends on  $T^*$ , viz.

$$x_c^* = -38.18 + 59.50T^* - 26.82T^{*2} + 4.21T^{*3} \quad (T^* > 1.2).$$

The inflection point of this curve occurs at  $T^* = 2.2$ , which separates the asymmetric wake and the coupled-street regime.

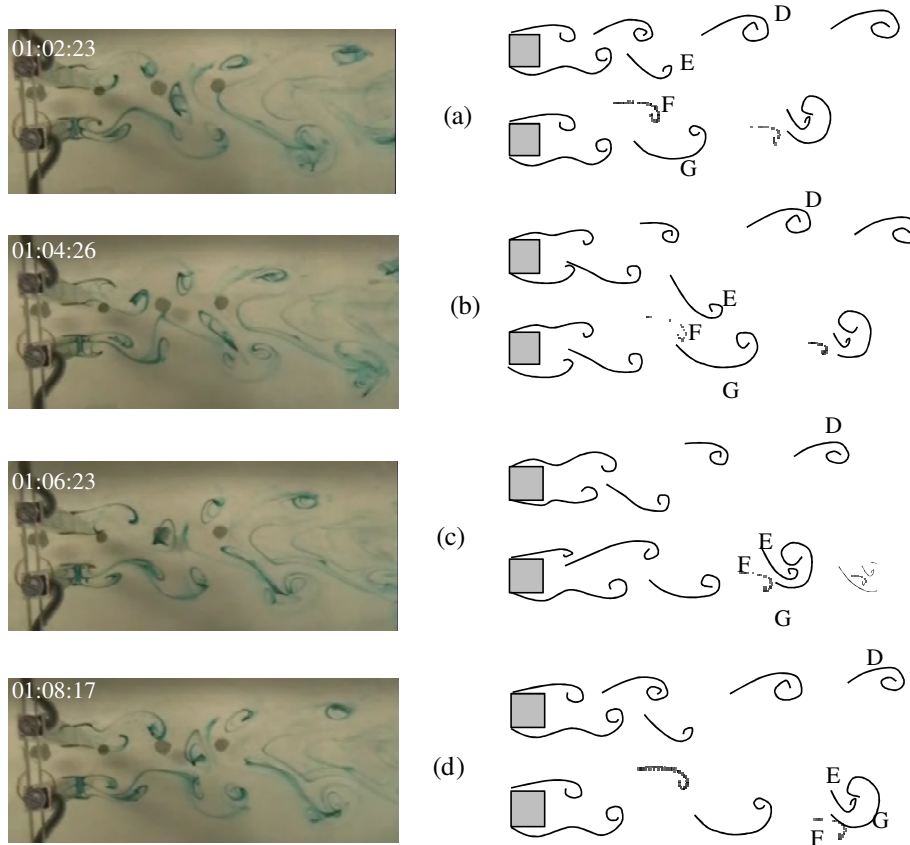


**Fig. 6.** Photographs and sketches showing the merge of two coupled streets into one.  $T^* = 2.75$ .

## 5. Acknowledgement

Alam wishes to acknowledge supports given to him from Shenzhen Government through grant CB24405004 and from China Govt through '1000-young-talent-program'.

## 6. References

- [1] M. Kiya, M. Arie, and H. Mori, "Vortex Shedding from Two Circular cylinders in Staggered Arrangement", *ASME Journal of Fluids Engineering*, Vol. 102, 166-173, 1980.
- [2] M.M. Alam, Y. Zhou, and X.W. Wang, "The Wake of Two Side-by-Side Square Cylinders", *Journal of Fluid Mechanics*, Vol. 669, 432-471, 2011.
- [3] H. Sakamoto, and H. Haniu, "Effect of Free Stream Turbulence on Characteristics of Fluctuating Forces Acting on Two Square Prisms in Tandem Arrangement," *ASME Journal of Fluids Engineering*, Vol. 110, 140-146, 1988.
- [4] V. Kolář, D.A. Lyn, and W. Rodi, "Ensemble-Averaged Measurements in the Turbulent Near Wake of Two Side-by-Side Square Cylinders," *Journal of Fluid Mechanics*, Vol. 346, 201-237, 1997.
- [5] A. Agarwal, L. Djenidi, and R.A. Antonia, "Investigation of Flow Around a Pair of Side-by-Side Square Cylinders using the Lattice Boltzmann Method," *Computer and Fluids*, Vol. 35, 1093-1107, 2006.
- [6] Y. Couder, and C.B. Basdevant, C. B., "Experimental and Numerical Study of Vortex Couples in Two-Dimensional Flows," *Journal of Fluid Mechanics*, Vol. 173, 225-251, 1986.